Available online at www.sciencedirect.com
SCIENCE DIRECT®
International Journal of Heat and Mass Transfer 48 (2005) 1739–1746
International Journal of HEAT and MASS TRANSFER
www.elsevier.com/locate/ijhmt

Analysis of flexible microchannel heat sink systems

K. Vafai *, A.-R.A. Khaled

Department of Mechanical Engineering, University of California, Riverside, A363 Bourns Hall, Riverside, CA 92521 0425, United States

Received 25 September 2004; received in revised form 19 November 2004

Abstract

In this work, single layered (SL) and double layered (DL) flexible microchannel heat sinks are analyzed. The deformation of the supporting seals is related to the average internal pressure by theory of elasticity. It is found that sufficient cooling can be achieved using SL flexible microchannel heat sinks at lower pressure drop values for softer seals. Double layered flexible microchannel heat sinks provide higher rate of cooling over SL flexible microchannel heat sinks at the lower range of pressure drops. Single layered flexible microchannel heat sinks are preferred for large pressure drop applications while DL flexible microchannel heat sinks are preferred for applications involving low pressure drops.

Keywords: Microchannel; Heat sink; Heat transfer; Seals; Single layer; Double layer

1. Introduction

The rapid development of microelectronics has created a need for large integration density of chips in digital devices such as VLSI components. These devices require increased current–voltage handling capabilities leading to large amount of dissipated heat within a small space. Microchannel heat sinks are one of the proposed methods that can be used to remove this excessive heating.

Microchannels have a very high heat transfer coefficient. Early works on microchannel heat sinks [1] had shown that parallel micro passages with 50 μm wide and 302 μm deep had thermal resistances as low as 9×10^{-6} K W^{-1} m^{-2}. This value is substantially lower than the conventional channel sized heat sinks [2–4]. Microchannel heat sink devices can be used as single layered (SL) micro passage such as those illustrated in the works of Lee and Vafai [5] and Fedorov and Viskanta [6]. Double layered (DL) microchannel heat sinks were introduced for the first time in the work of Vafai and Zhu [7] to provide additional cooling capacity for the microchannel and to decrease the axial temperature gradients along the microchannel. Single layered microchannel heat sinks can be either single channel system such as those analyzed in the work of Harms et al. [8] or multiple channel system [5].

One of the drawbacks of microchannel heat sinks is the increased temperature of the coolant as large amount of heat is carried out by a relatively small amount of coolant. As such, new technologies developed in the works of Vafai and Zhu [7] and Khaled and Vafai [9–11] provide new solutions for cooling of electronic components utilizing microchannel heat sinks. The work of Khaled and Vafai [9–11] is based on utilizing flexible soft seals. The resulting microchannel heat sink system is referred to as ''flexible microchannel heat sink''. Khaled

* Corresponding author. Tel.: +1 951 827 2135; fax: +1 951 827 2899.
E-mail address: vafai@engr.ucr.edu (K. Vafai).

0017-9310/$ - see front matter © 2005 Elsevier Ltd. All rights reserved.
doi:10.1016/j.ijheatmasstransfer.2004.11.020

Nomenclature

B	microchannel length [m]
c_p	specific heat of the coolant [J kg^{-1} K^{-1}]
W	width of the microchannel [m]
F	fixation parameter defined in Eq. (9)
F_{critical}	critical fixation parameter defined in Eq. (19)
H	microchannel thickness [m]
H_0	reference microchannel thickness [m]
h_c	convective heat transfer coefficient [W m^{-2} K]
K	effective stiffness of the seal [N m^{-1}]
k	thermal conductivity of the fluid [W m^{-1} K^{-1}]
M	dimensionless delivered coolant mass flow rate defined on Eq. (29)
m	dimensional delivered coolant mass flow rate [kg m^{-1} s^{-1}]
Nu	lower plate's Nusselt number defined on Eq. (16)
Pr	Prandtl number $\mu c_p/k$
p	fluid pressure [N m^{-2}]
q	heat flux at the lower plate [W m^{-1}]
Re	Reynolds number, $\rho u_m H/\mu$
$(Re)_{\text{critical}}$	critical Reynolds number defined in Eq. (20)
Re_0	dimensionless pressure drop, $\rho u_m H_0/\mu$
$(Re_0)_{\text{SL}}$	dimensionless pressure drop for single layered flexible microchannel
$(Re_0)_{\text{DL}}$	dimensionless pressure drop for double layered flexible microchannel
T, T_1	temperature in fluid and the inlet temperature [K]
U	dimensionless axial velocities, u/u_m
u	dimensional axial velocities [m s^{-1}]
u_m	average axial velocity [m s^{-1}]
U_F	uncertainty in mean bulk temperature with respect to F defined in Eq. (14)
U_{Re_0}	uncertainty in mean bulk temperature with respect to Re_0 defined in Eq. (13)
X	dimensionless axial coordinates, x/H
x	dimensional axial coordinates [m]
Y	dimensionless normal coordinates, y/H
y	dimensional normal coordinates [m]

Greek symbols

ε	perturbation parameter, H/B
$\varepsilon_{\text{critical}}$	critical perturbation parameter defined in Eq. (21)
ε_0	reference perturbation parameter, H_0/B
γ	friction force ratio defined in Eq. (29)
κ_m	mean bulk temperature ratio defined in Eq. (25)
κ_W	heated plate temperature ratio defined in Eq. (26)
μ	dynamic viscosity of the fluid
θ	dimensionless temperature, $(T - T_1)/(qH/k)$
θ_m	dimensionless mean bulk temperature, $(T_m - T_1)/(qH/k)$
θ_W	dimensionless temperature at the heated plate, $(T_W - T_1)/(qH/k)$
θ^*	temperature normalized with reference conditions defined in Eq. (10)
ρ	density of the fluid

and Vafai [9] demonstrated that additional cooling can be achieved if flexible thin films including flexible microchannel heat sinks are utilized. In this work, the expansion of the flexible thin film including flexible microchannel heat sink is directly related to the internal pressure. Khaled and Vafai [10] have demonstrated that significant cooling inside flexible thin films can be achieved if the supporting seals contain closed cavities which are in contact with the heated surface. They referred to this kind of sealing assembly as "flexible complex seals". Moreover, Khaled and Vafai [11] demonstrated that flexible complex seals along with thin films have important applications in design and control of the flow and thermal characteristics of these types of systems.

In this work, the enhancement in the cooling process inside SL and DL flexible microchannel heat sinks is investigated. The theory of linear elasticity applied to the supporting seals is utilized to relate the average internal pressure to the thickness of the flexible microchannel heat sinks. The resulting equations are then solved numerically and analytically to determine the effects of the pressure drop, softness of the supporting seals, the Prandtl number and the coolant mass flow rate on the thermal characteristics of both SL and DL flexible microchannel heat sinks.

2. Problem formulation

2.1. Single layered flexible microchannel heat sinks

Consider flow inside a two dimensional microchannel heat sink with a height H and axial length B. The x-axis

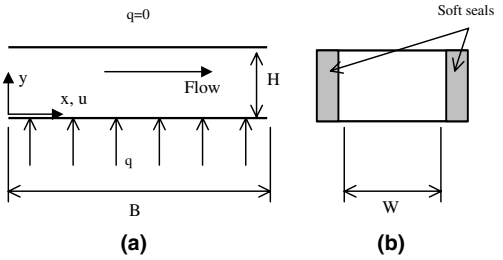

Fig. 1. Schematic diagram and the coordinate system for the proposed single layered flexible microchannel heat sink: (a) front view, and (b) side view.

is aligned along the channel length while the y-axis is in the traverse direction as shown in Fig. 1. The fluid is taken to be Newtonian with constant average properties. Using the following dimensionless variables:

$$X = \frac{x}{B}, \quad Y = \frac{y}{H}, \quad U = \frac{u}{u_{\mathrm{m}}}, \quad \theta = \frac{T - T_1}{qH/k} \tag{1}$$

leads to the following dimensionless energy equation:

$$Re\,Pr\varepsilon U\frac{\partial\theta}{\partial X} = \frac{\partial^2\theta}{\partial Y^2} \tag{2}$$

where q, T_1 and Re are the heat flux at the heated plate, the inlet temperature and the Reynolds number ($Re = (\rho u_{\mathrm{m}} H)/\mu$), respectively. Pr and ε are the Prandtl number ($Pr = \upsilon/\alpha$) and the perturbation parameter ($\varepsilon = H/B$). The mean velocity is related to the pressure drop across the channel, Δp, through the following relation (assuming fully developed laminar flow conditions):

$$u_{\mathrm{m}} = \frac{1}{12\mu}\frac{\Delta p}{B}H^2 \tag{3}$$

where μ is the dynamic viscosity of the coolant.

For microchannel heat sinks supported by flexible soft seals, the separation between the microchannel's plates can be expressed according the following assuming that the seals are linear elastic materials:

$$H = H_0 + \frac{\Delta pBW}{2K} \tag{4}$$

where H_0, W and K are a reference thickness of the microchannel heat sink, the width of the microchannel heat sink and the stiffness of the supporting seal, respectively. As such, the Reynolds number and the perturbation parameter can be expressed according to the following relations:

$$Re = Re_0(1 + Re_0F)^3 \tag{5}$$

$$\varepsilon = \varepsilon_0(1 + Re_0F) \tag{6}$$

where Re_0 and ε_0 are the Reynolds number and the perturbation parameter evaluated at the reference microchannel thickness and the parameter F is the fixation parameter. These parameters are defined as

$$Re_0 = \frac{\rho}{12\mu^2}\frac{\Delta p}{B}H_0^3 \tag{7}$$

$$\varepsilon_0 = \frac{H_0}{B} \tag{8}$$

$$F = \frac{6\mu^2B^2W}{\rho KH_0^4} \tag{9}$$

The parameter Re_0 can be interpreted as the dimensionless pressure drop parameter. The temperature normalized with respect to the reference parameters, θ^* is defined as follows

$$\theta^* = \frac{T - T_1}{qH_0/k} \tag{10}$$

The normalized mean bulk temperature, obtained from the solution of integral form of Eq. (2) is

$$(\theta^*)_{\mathrm{m}} = \frac{X}{Pr\,Re_0\varepsilon_0(1 + Re_0F)^3} \tag{11}$$

The uncertainty in $(\theta^*)_{\mathrm{m}}$, $\Delta(\theta^*)_{\mathrm{m}}$, is

$$U_{(\theta^*)_{\mathrm{m}}} = \Delta(\theta^*)_{\mathrm{m}} = U_{Re_0}\Delta Re_0 + U_F\Delta F \tag{12}$$

where U_{Re_0} and U_F are defined as

$$U_{Re_0} = \frac{\partial(\theta^*)_{\mathrm{m}}}{\partial Re_0} = -\frac{(1 + 4Re_0F)X}{Pr\,Re_0^2\varepsilon_0(1 + Re_0F)^4} \tag{13}$$

$$U_F = \frac{\partial(\theta^*)_{\mathrm{m}}}{\partial F} = -\frac{3X}{Pr\varepsilon_0(1 + Re_0F)^4} \tag{14}$$

2.2. Boundary conditions

The lower plate is assumed to have a uniform wall heat flux and the upper plate is considered to be insulated. As such the dimensionless boundary conditions can be written as

$$\theta(0, Y) = 0, \quad \frac{\partial\theta(X, 0)}{\partial Y} = -1, \quad \frac{\partial\theta(X, 1)}{\partial Y} = 0 \tag{15}$$

The Nusselt number is defined as

$$Nu = \frac{h_cH_0}{k} = \frac{1}{(\theta^*)_{\mathrm{W}} - (\theta^*)_{\mathrm{m}}} = \frac{1}{\theta^*(X, 0) - (\theta^*)_{\mathrm{m}}} \tag{16}$$

where $(\theta^*)_{\mathrm{W}}$ is the heated plate temperature normalized with respect to the reference parameters. Under fully developed thermal conditions, Nusselt number approaches the following value:

$$Nu = \frac{h_cH_0}{k} = \frac{2.69}{1 + Re_0F} = \frac{1}{(\theta^*)_{\mathrm{W}} - (\theta^*)_{\mathrm{m}}} \tag{17}$$

where $(\theta^*)_{\mathrm{W}}$ is the dimensionless lower plate temperature under fully developed thermal conditions. Thus, it can be expressed according to the following:

$$[(\theta^*)_W]_{fd} = \frac{1 + Re_0 F}{2.69} + \frac{X}{Pr\, Re_0 \varepsilon_0 (1 + Re_0 F)^3} \tag{18}$$

Minimizing this temperature at the exit results in the following value of the fixation parameter

$$\frac{\partial[(\theta^*)_W]_{fd}}{\partial F} = 0 \;\Rightarrow\; F_{critical} = \frac{1.685}{(Re_0\, Pr\varepsilon_0)^{1/4} Re_0} - \frac{1}{Re_0} \tag{19}$$

As such, the corresponding Reynolds number and the perturbation parameters are

$$(Re)_{critical} = 4.784 \left(\frac{Re_0}{(Pr\varepsilon_0)^3} \right)^{1/4} \tag{20}$$

$$(\varepsilon_0)_{critical} = 1.685 \left(\frac{\varepsilon_0^3}{Re_0\, Pr} \right)^{1/4} \tag{21}$$

2.3. Double layered flexible microchannel heat sinks

Fig. 2 shows the proposed two layered (DL) flexible microchannel heat sink with counter flow as proposed by Vafai and Zhu [7]. The governing energy equations for both layers are

$$Re_0\, Pr\varepsilon_0 (1 + Re_0 F)^4 U(Y_1) \frac{\partial \theta_1}{\partial X_1} = \frac{\partial^2 \theta_1}{\partial Y_1^2} \tag{22}$$

$$Re_0\, Pr\varepsilon_0 (1 + Re_0 F)^4 U(Y_2) \frac{\partial \theta_2}{\partial X_2} = \frac{\partial^2 \theta_2}{\partial Y_2^2} \tag{23}$$

where the subscripts 1 and 2 are for the lower and the upper layers, respectively.

The corresponding boundary conditions are

$$\theta_1(X_1 = 0, Y) = \theta_2(X_2 = 0, Y) = 0, \quad \frac{\partial \theta_1(X_1, 0)}{\partial Y_1} = -1$$
$$\frac{\partial \theta_1(X_1, 1)}{\partial Y_1} = \frac{\partial \theta_2(X_2 = 1 - X_1, 0)}{\partial Y_2}, \quad \frac{\partial \theta_2(X_2, 1)}{\partial Y_2} = 0 \tag{24}$$

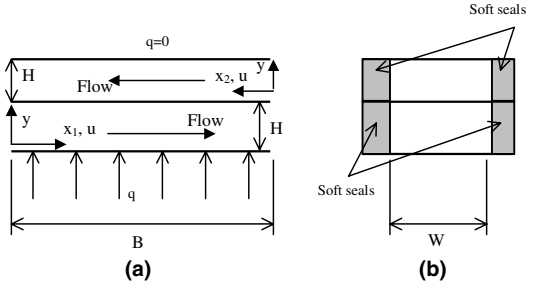

Fig. 2. Schematic diagram and the coordinate system for the proposed double layered flexible microchannel heat sink: (a) front view, and (b) side view.

The intermediate plate is taken to be made from a highly conductive material like copper such that temperature variation across this plate is negligible. The following parameters are introduced in order to compare the performance of the DL flexible microchannel heat sink compared to SL flexible microchannel heat sink:

$$\kappa_m = \frac{[\theta^*_{m1}(X_1 = 1)]_{DL}}{[\theta^*_m(X = 1)]_{SL}} \tag{25}$$

$$\kappa_W = \frac{[(\theta^*_W)_{AVG}]_{DL}}{[(\theta^*_W)_{AVG}]_{SL}} \tag{26}$$

Lower values of the cooling factors κ_m and κ_W indicate that DL flexible microchannel heat sinks are preferable over SL flexible microchannel heat sinks.

Another factor that will be considered is the ratio of the total friction force in DL flexible microchannel heat sinks to that for SL flexible microchannel heat sinks delivering the same flow rate of coolant. It can be shown that this factor is equal to

$$\gamma \equiv \frac{(\text{Friction force})_{DL}}{(\text{Friction force})_{SL}} = \frac{2(\Delta p)_{DL} H_{DL}}{(\Delta p)_{SL} H_{SL}} = \frac{2(Re_0)_{DL}(1 + (Re_0)_{DL} F)}{(Re_0)_{SL}(1 + (Re_0)_{SL} F)} \tag{27}$$

where $(Re_0)_{DL}$ and $(Re_0)_{SL}$ are related through the following:

$$(Re_0)_{DL}(1 + (Re_0)_{DL} F)^3 = 2(Re_0)_{SL}(1 + (Re_0)_{SL} F)^3 \tag{28}$$

As such, the delivered dimensionless mass flow rate by both SL and DL flexible microchannel heat sinks is

$$M = \frac{m}{\mu} = \frac{(2\rho u_m H)}{\mu} = 2(Re_0)_{DL}(1 + (Re_0)_{DL} F)^3 \tag{29}$$

where m is the dimensional mass delivered by both flexible microchannel heat sinks.

3. Numerical analysis

Eqs. (2), (22) and (23) were descritized using three points central differencing in the transverse direction while backward differencing was utilized for the temperature gradient in the axial direction. The resulting tridiagonal system of algebraic equations at $X = \Delta X$ was then solved using the well established Thomas algorithm [12]. The same procedure was repeated for the consecutive X-values until X reached the value of unity. For Eqs. (22) and (23), the temperature distribution at the intermediate plate was initially prescribed. Eqs. (22) and (23) were solved as described before. The thermal boundary condition at the intermediate plate was then used to correct for intermediate plate temperatures.

The procedure was repeated until all the thermal boundary conditions were satisfied.

In most of the cases considered here, the minimum value of Re was taken to be 50 while the maximum Re value was allowed to expand to 2100 for $Re_0 = 50$ and $F = 0.05$. The maximum Re corresponded to a microchannel heat sink that was substantially expanded due to the presence of soft seals. The thickness for the latter limiting case ($Re = 2100$) was found to be 3.5 times the thickness of the former limiting case ($Re = 50$). The maximum fixation parameter was taken to be 0.05. This represented a thin film microchannel heat sink filled with water, having $B = 60$ mm, $W = 20$ mm, $h_0 = 0.3$ mm, and $K = 1000$ N/m.

4. Discussions of results

4.1. Effects of fixation parameter and pressure drop on the thermal behavior of SL flexible microchannel heat sinks

Figs. 3 and 4 illustrate effects of the fixation parameter F and the dimensionless pressure drop Re_0 on the mean bulk temperature at the exit and the average heated plate temperature for SL flexible microchannel heat sinks, respectively. As the seal become softer, the fixation parameter increases allowing for further expansion of the microchannel at a given dimensionless pressure drop, Re_0. Thus, the mean bulk temperature is further reduced as shown in Fig. 3 and the heated plate is further cooled as shown in Fig. 4 due to an increase in the coolant flow rate. As seen in Fig. 4, relatively low pressure drop is capable of producing efficient cooling compared to that at larger pressure drops for larger F values.

Convective heat transfer coefficient is reduced as F increases at low dimensionless pressure drops as shown in Fig. 5. This is because coolant velocities decrease near the heated plate as F increases. However, for larger pressure drops, flow increases due to both an increase in the pressure drop and the expansion of the microchannel as F increases resulting in an increase in the thermal developing region effects. As such, the convective heat transfer coefficient increases as F increases for larger Re_0 and F values as illustrated in Fig. 5. Fig. 6 shows that the mean bulk temperature becomes less sensitive to the dimensionless pressure drop Re_0 and the fixation parameter F as both F and Re_0 increase.

Fig. 7 demonstrates that flexible microchannel heat sinks operating at lower Reynolds numbers possess lower heated plate temperature at the exit as F increases. This is not seen when these heat sinks are operated at higher Reynolds number values. As such, the enhancement in the cooling process using flexible microchannel

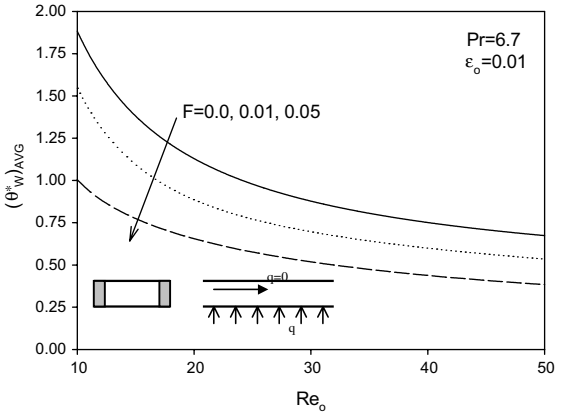

Fig. 4. Effects of the pressure drop ($Re_0 = \frac{\rho}{12\mu^2}\frac{\Delta p}{B}H_0^3$) on the dimensionless average lower plate temperature for a single layer flexible microchannel heat sink.

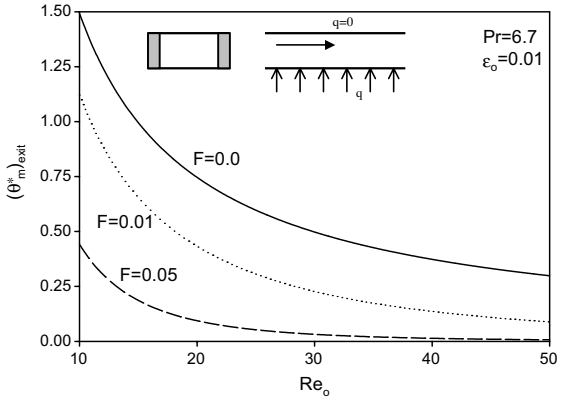

Fig. 3. Effects of the pressure drop $\left(Re_0 = \frac{\rho}{12\mu^2}\frac{\Delta p}{B}H_0^3\right)$ on the dimensionless exit mean bulk temperature for a single layer flexible microchannel heat sink.

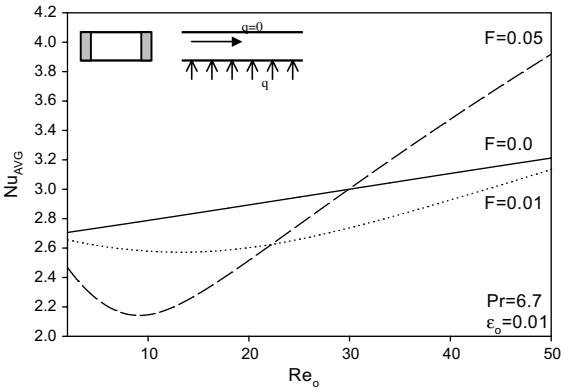

Fig. 5. Effects of the pressure drop ($Re_0 = \frac{\rho}{12\mu^2}\frac{\Delta p}{B}H_0^3$) on the dimensionless average convective heat transfer coefficient for a single layer flexible microchannel heat sink.

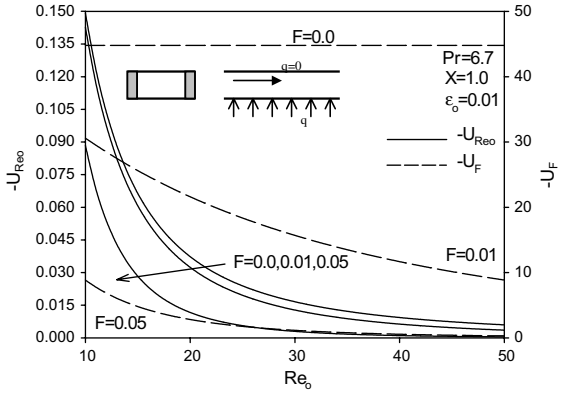

Fig. 6. Effects of the pressure drop ($Re_0 = \frac{\rho}{12\mu^2}\frac{\Delta p}{B}H_0^3$) on U_{Re_0} and U_F for a single layer flexible microchannel heat sink.

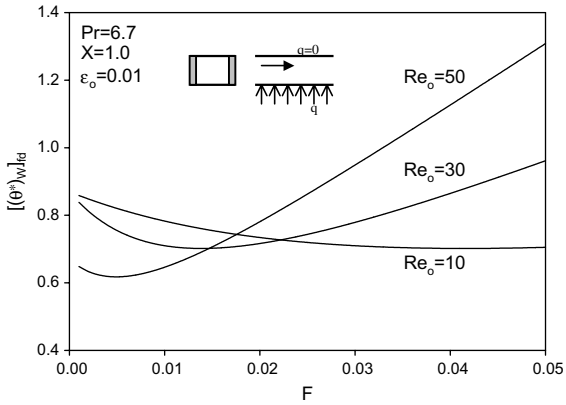

Fig. 7. Effects of the fixation parameter on the fully developed heated plate temperature at the exit for a single layer flexible microchannel heat sink.

heat sinks is not significant at large pressure drops as illustrated in Fig. 4.

4.2. Effects of fixation parameter and Prandtl number on thermal behavior of SL flexible microchannel heat sinks

Fig. 8 illustrates the effects of the fixation parameter F and Prandtl number Pr on the average heated plate temperature for SL flexible microchannel heat sinks. As seen in Fig. 8, sufficient increase in the cooling effect can be achieved by increasing F as Pr decreases. This is mainly due to an increase in the coolant flow rate as F increases. On the other hand, convective heat transfer coefficient is reduced as F increases at low Pr values as shown in Fig. 9. This is because coolant velocities decrease near the heated plate as F increases. As seen in Fig. 9, for large Pr values, thermal developing region effects increase causing the convective heat transfer coefficient to increase as F increases.

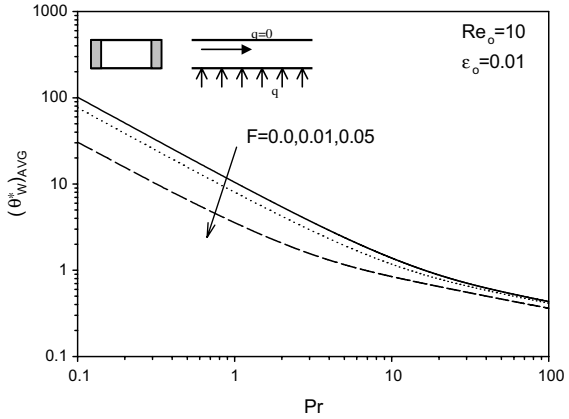

Fig. 8. Effects of Prandtl number on the dimensionless average lower plate temperature for a single layer flexible microchannel heat sink.

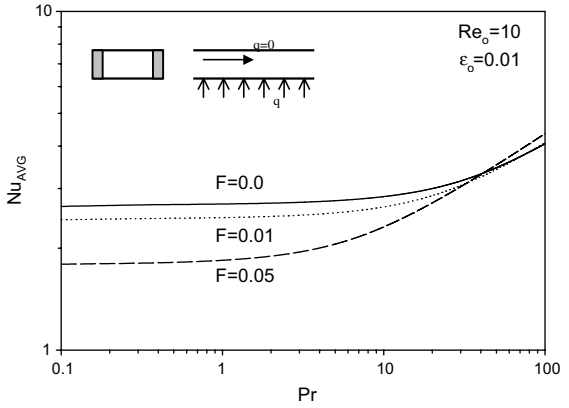

Fig. 9. Effects of Prandtl number on the average convective heat transfer coefficient for a single layer flexible microchannel heat sink.

4.3. Effects of fixation parameter and pressure drop on thermal behavior of DL flexible microchannel heat sinks

Fig. 10 describes the axial behavior of the mean bulk temperature for two different DL flexible microchannel heat sinks having different fixation parameters. Additional cooling is achieved by introducing the secondary layer which can be seen in Fig. 10 for the case with $F = 0.01$. This plot shows that the maximum coolant temperature occurs before the exit unlike SL flexible microchannel heat sinks where this temperature occurs at the exit. As F increases, convection increases in the main layer while conduction to the upper layer decreases. This is due to an increase in the convective heat transfer and an increase in the expansion of the main layer. As such, the increase in the cooling capacity of DL flexible microchannel heat sinks becomes insignifi-

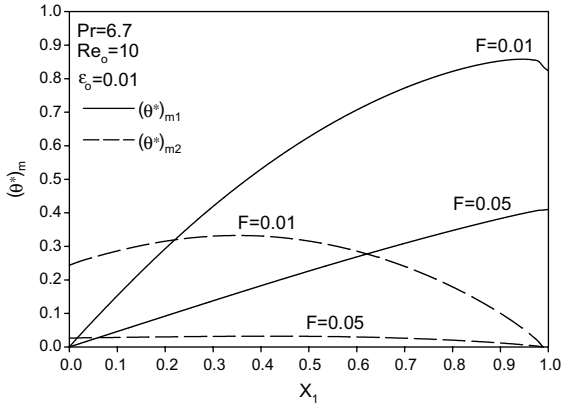

Fig. 10. Effects of the fixation parameter on the mean bulk temperature inside the double layered flexible microchannel heat sink.

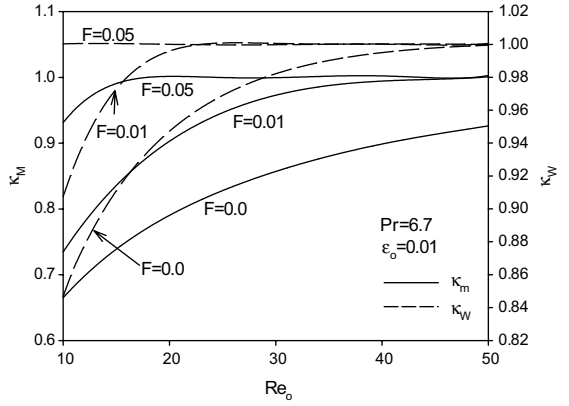

Fig. 11. Effects of the pressure drop $(Re_0 = \frac{\rho}{12\mu^2}\frac{\Delta p}{B}H_0^3)$ on κ_m and κ_W.

cant at both large values of the pressure drop and the fixation parameter. This fact is clearly seen in Fig. 11 where the heated plate temperature for DL flexible microchannel heat sinks are almost the same as that for the SL flexible microchannel heat sinks with $F = 0.05$ for a wide range of Re_0. Note that κ_m is the ratio of the mean bulk temperature at the exit for DL flexible microchannel to that for *SL* flexible microchannel heat sink. The parameter κ_W is the ratio of the average heated plate temperature for DL flexible microchannel to that for SL flexible microchannel heat sink.

4.4. Comparisons between SL and DL flexible microchannel heat sinks delivering the same coolant flow rates

Fig. 12 shows the effect of the fixation parameter F and the dimensionless pressure drop for DL flexible

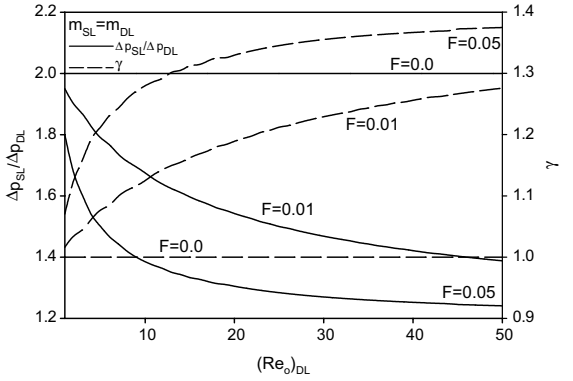

Fig. 12. Effects of the pressure drop $((Re_0)_{DL} = \frac{\rho}{12\mu^2}\frac{(\Delta p)_{DL}}{B}H_0^3)$ on the pressure drop ratio and the friction force ratio between single and double layered flexible microchannel heat sinks.

microchannel heat sinks on the pressure drop and friction force ratios between SL and DL flexible microchannel heat sinks. These microchannel heat sinks are considered to deliver the same coolant flow rate. As F increases, the pressure drop in SL flexible microchannel heat sinks required to deliver the same flow rate as for the DL flexible microchannel heat sinks decreases. This value is further decreased as the pressure drop in DL flexible microchannel heat sink increases. Meanwhile, as F increases, the ratio of the friction force encountered in the proposed DL flexible microchannel heat sink to that associated with the SL flexible microchannel heat sink increases. This indicates that SL flexible microchannel heat sinks delivering the same flow rate as for DL microchannel heat sinks having the same F value encounter fewer friction losses.

Fig. 13 demonstrates that SL flexible microchannel heat sinks can provide better cooling attributes compared to DL flexible microchannel heat sinks delivering the same coolant flow rate and having the same F values.

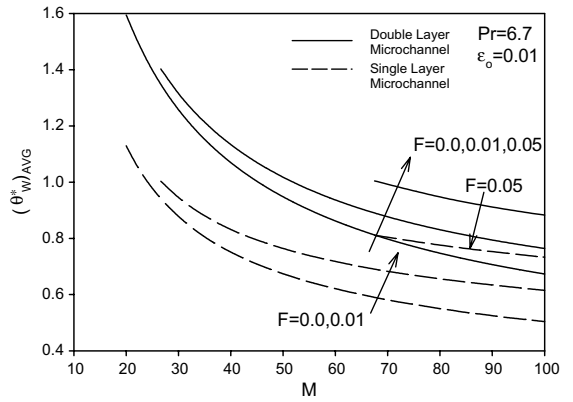

Fig. 13. Effects of the delivered coolant mass flow rate on the average heated plate temperature for both single and double layered flexible microchannel heat sinks.

However; note that rigid DL microchannel heat sinks provides better cooling than rigid SL microchannel heat sinks when operated at the same pressure drop as shown in Fig. 11. It should be noted that Fig. 13 shows that microchannel heat sinks with stiffer seals provide additional cooling over those with softer seals delivering the same flow rate. This is because the former are thinner and have larger velocities than the latter microchannel heat sinks. As such, convective heat transfer for rigid microchannels will be higher than that for flexible microchannel heat sinks delivering the same flow rate.

5. Conclusions

Heat transfer inside SL and DL flexible microchannel heat sinks have been analyzed in this work. The deformation of the supporting seals was related to the average internal pressure by theory of linear elasticity. Increases in the fixation parameter and the dimensionless pressure drop were found to cause enhancements in the cooling process. These enhancements are significant at lower pressure drop values. Moreover, DL flexible microchannel heat sinks were found to provide additional cooling which were significant at lower values of pressure drop for stiff seals. It is preferred to utilize SL flexible microchannel sinks over DL microchannel heat sinks for large pressure drop applications. However, at lower flow rates the DL flexible microchannel heat sink is preferred to be used over SL flexible microchannel heat sinks especially when stiff sealing material is utilized.

Acknowledgment

We acknowledge partial support of this work by DOD/DARPA/DMEA under grant number DMEA90-02-2-0216.

References

[1] D.B. Tuckerman, D.B. Pease, High-performance heat sinking for VLSI, IEEE Electron Dev. Lett. EDL-2 (1981) 126–129.
[2] L.J. Missaggia, J.N. Walpole, Z.L. Liau, R.J. Philips, Microchannel heat sinks for two dimensional high-power-density diode laser arrays, IEEE J. Quantum Electron. 25 (1989) 1988–1992.
[3] M.B. Kleiner, S.A. Kuhn, K. Haberger, High performance forced air cooling scheme employing micro-channel heat exchangers, IEEE Trans. Compon. Pack. Manuf. Technol. Part A 18 (1995) 795–804.
[4] V.K. Samalam, Convective heat transfer in micro-channels, J. Electron. Mater. 18 (1989) 611–617.
[5] D.Y. Lee, K. Vafai, Comparative analysis of jet impingement and microchannel cooling for high heat flux applications, Int. J. Heat Mass Transfer 42 (1999) 1555–1568.
[6] A.G. Fedorov, R. Viskanta, Three-dimensional conjugate heat transfer in the microchannel heat sink for electronic packaging, Int. J. Heat Mass Transfer 43 (2000) 399–415.
[7] K. Vafai, L. Zhu, Analysis of a two-layered micro channel heat sink concept in electronic cooling, Int. J. Heat Mass Transfer 42 (1999) 2287–2297.
[8] T.M. Harms, M.J. Kazmierczak, F.M. Gerner, Developing convective heat transfer in deep rectangular microchannels, Int. J. Heat Fluid Flow 20 (1999) 149–157.
[9] A.-R.A. Khaled, K. Vafai, Flow and heat transfer inside thin films supported by soft seals in the presence of internal and external pressure pulsations, Int. J. Heat Mass Transfer 45 (2002) 5107–5115.
[10] A.-R.A. Khaled, K. Vafai, Cooling enhancements in thin films supported by flexible complex seals in the presence of ultrafine suspensions, ASME J. Heat Transfer 125 (2003) 916–925.
[11] A.-R.A. Khaled, K. Vafai, Control of exit flow and thermal conditions using two-layered thin films supported by flexible complex seals, Int. J. Heat Mass Transfer 47 (2004) 1599–1611.
[12] F.G. Blottner, Finite-difference methods of solution of the boundary-layer equations, AIAA J. 8 (1970) 193–205.